Aircraft-based observations of cirrus mid- and far-infrared radiative signatures during the Cirrus Coupled Cloud Radiation Experiment

Richard Bantges[1], Helen Brindley[1], Jonathan Murray[1], Caroline Cox[2] , Caroline Poulsen[2], & CIRCCREX Team

1:Space and Atmospheric Physics, Imperial College London and NERC National Centre for Earth Observation

2: RAL Space, Science and Technology Facilities Council, UK Research and Innovation

ABSTRACT

We describe efforts that are underway to assess the performance of recently developed ice cloud bulk scattering models using measurements of nadir radiances from 100-3000 cm^{-1} obtained from the UK Facility for Airborne Atmospheric Measurements (FAAM) BAe-146 aircraft during the Cirrus Coupled Cloud-Radiation Experiment (CIRCCREX). Preliminary results suggest that the far- infrared observations can provide a means to discriminate between bulk scattering models which are all able to satisfactorily match mid- infrared observations due to their enhanced sensitivity to crystal habit.

INTRODUCTION

This poster provides a brief summary of the relevant data obtained during flight B895 as part of the CIRCCREX campaign, and the methods and tools used to simulate some of those observations. Two different approaches are taken: the initial stage of the work involves forward modelling of the observed radiances using measurements of the atmospheric state, with a particular emphasis on assessing consistency between our ability to capture mid- and far- infrared behaviour. A second complementary activity aims to develop an inverse modelling capability to assess whether the far infrared observations provide additional information, particularly concerning the cirrus microphysics, compared to that available from the mid- infrared.

CIRCCREX CAMPAIGN: FAAM Flight B895 Summary

Taking off from Prestwick in the UK on the 13th March 2015, FAAM flight B895 overflew a decaying band of cirrus cloud associated with an occluded front. The main objective of the flight was to characterise both the cirrus microphysics and associated radiative signature across the electromagnetic spectrum. As such the aircraft performed straight and level runs (SLRs) above and within the cloud, as well as descending and ascending through the cloud layer. Note that since only a single aircraft platform was available the 'in-cloud' observations of cloud microphysics were not taken at a coincident time with the remote radiation measurements. Figure 1 shows the flight track for the entire flight, with the 3 SLRs of interest indicated in colour.

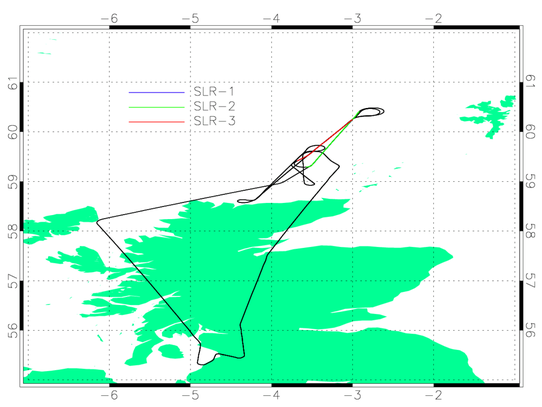

Figure 1: Flight track for FAAM Flight B895 shown in black. The 3 SLRs are shown in colour, but note that SLR-1 lies directly beneath SLR-2 and is therefore not visible.

The FAAM aircraft was fitted with a 'cloud-radiation' suite of instrumentation in addition to its core instrumentation that enabled the atmosphere immediately around the aircraft and also the cloud layer and underlying atmosphere to be characterised. These instruments included two Fourier transform spectrometers (FTS's): the Tropospheric Airborne Fourier Transform Spectrometer (TAFTS, Canas et al. 1997) with nominal spectral coverage from 80 cm^{-1} to 600 cm^{-1} at 0.12cm^{-1} resolution, and the Airborne Research Interferometer Evaluation System (ARIES, Wilson et al. 1999) with nominal spectral coverage from 550 cm to 3000 cm^{-1} at 1 cm^{-1} resolution. A Leosphere ALS450 355nm elastic backscatter lidar (Marenco 2010) was also fitted along with the standard aircraft positioning, temperature and humidity sensors and the Airborne Vertical Atmospheric Profiling System (AVAPS) [Vaisala, 1999]. Figure 2 indicates the times during the period around the 3 SLRs when radiance spectra from TAFTS and ARIES are available along with the times when the dropsondes were released from the aircraft.

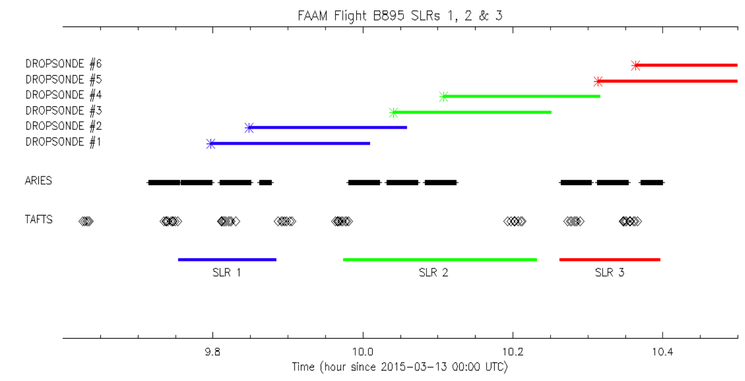

Figure 2: Summary of the availability of TAFTS and ARIES radiance spectra and dropsonde data. The timings of the 3 SLRs are shown for reference, and the release times for the dropsondes are indicated with an asterisk and colour-code indicating the SLR which they are associated with.

Figure 3 shows the Leosphere ALS450 lidar data from the 3 SLRs that has been processed to produce the atmospheric volume extinction coefficient as function of distance from the aircraft. This information can then be used to build a vertical profile of the cloud beneath the aircraft. Two lidar profiles, "CASE 1" & "CASE 3", have been identified as suitable preliminary case studies when coincident TAFTS and ARIES observations are available. These interferometer spectra are shown in figure 4, which highlights the variation between the two cases.

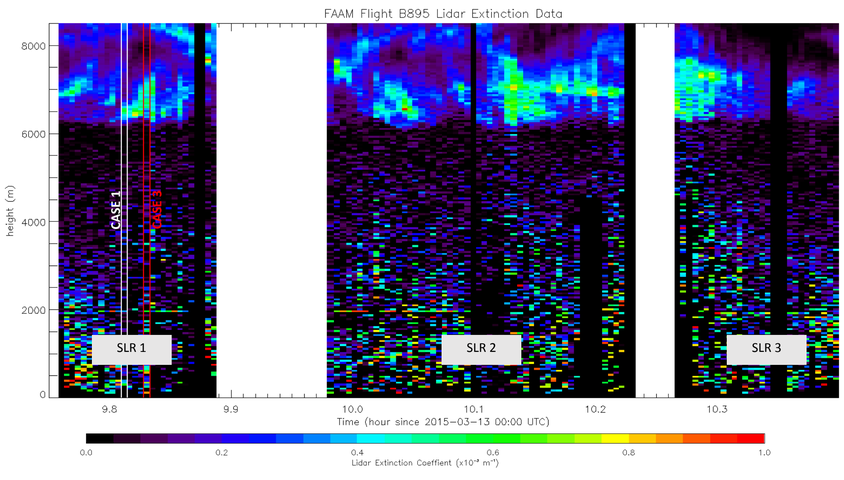

Figure 3: Vertical profile of the Lidar extinction coefficients processed from the backscatter lidar returns during the 3 SLRs for FAAM Flight B895.

CASE STUDIES 1 & 3: TAFTS and ARIES brightness temperature spectra from above a thin cirrus layer during SLR1

Three lidar profiles were identified from SLR1, when suitable coincident TAFTS and ARIES spectra were available, as potentially interesting case studies. However, upon further analysis, case 2 was found to be similar to case 1, hence only cases 1 & 3 are shown here. The objective was to assess the consistency of the simulated spectra between the mid- (ARIES) and far- (TAFTS) infrared using the available observational data and cirrus optical models.

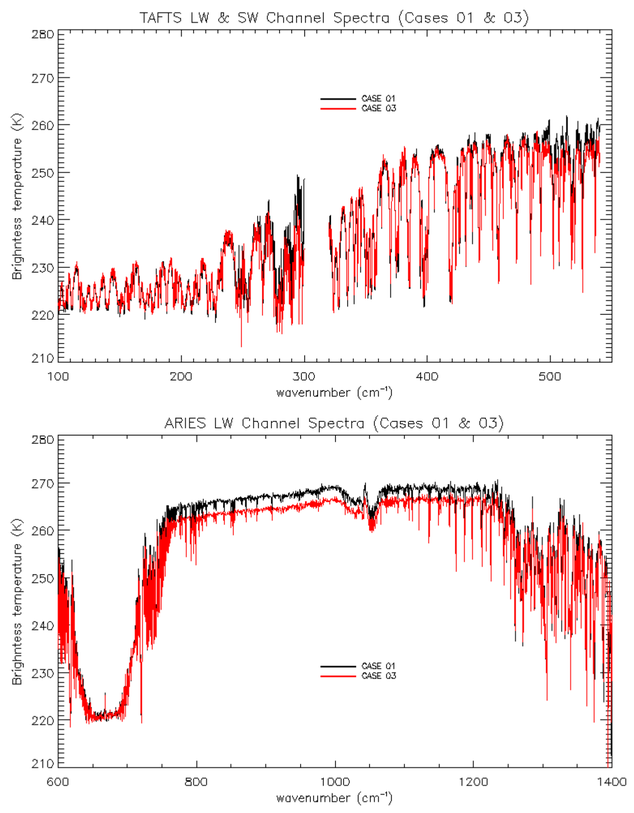

Figure 4: Upper: TAFTS longwave (LW) and shortwave (SW) channel equivalent brightness temperature spectra for cases 1 & 3 during SLR1 of FAAM flight B895. Lower: ARIES LW channel spectra.

Radiative Transfer Modelling of TAFTS & ARIES spectra

Data from the on-board aircraft instruments, combined with those from the dropsonde, lidar and ECMWF Operational Analyses, were used to define the atmospheric profile from the sea surface to the aircraft altitude at approximately 9.4 km above sea level, at 100 m vertical resolution. These data were then used as input to the Line-by-Line Radiative Transfer Model (LBLRTM) v12.8 to calculate the optical depth for each atmospheric layer, and subsequently LBLDIS v2.1 to calculate radiance spectra at the aircraft altitude. These spectra were then convolved with the relevant TAFTS and ARIES instrument functions. A schematic of the processing is shown in figure 5.

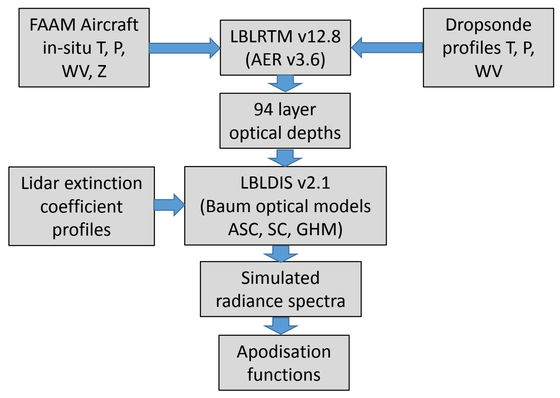

Figure 5: Schematic summarising the processing steps to produce simulated TAFTS and ARIES radiance spectra.

Figure 6 shows the dropsonde profiles, interpolated to 100 m vertical resolution, of temperature and water vapour for those two dropsondes released closest in time to cases 1 & 3, as well as the two lidar extinction coefficient profiles. ECMWF Operational Analyses data were obtained to provide estimates of the ozone column profile, surface temperature and wind speed. The sea surface emissivity was characterised using the wind speed dependent model of Masuda (1988).

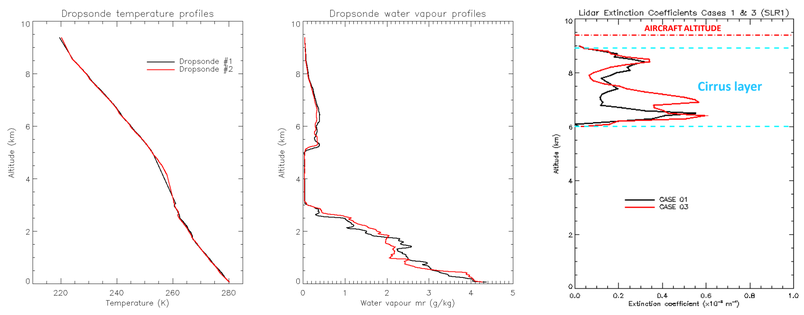

Figure 6: Dropsonde profiles of temperature (left) and water vapour (centre) for the two dropsondes released in SLR1. Right: Lidar extinction coefficient profiles (defined at 355nm) for the two case studies with the cloud vertical extents and approximate aircraft altitude shown.

Cirrus cloud in-situ properties & optical models

In-situ cloud microphysical properties of the decaying band of cirrus were measured after the completion of the 3 SLRs using a range of optical probes. A summary of these and their results is reported in O'Shea 2016. They indicate particle size distributions with a mean effective diameter ranging from around 80 to 200 µm. For the simulations reported here, the Baum (2014) ice cloud optical property models have been used. These provide single scattering properties for 3 different crystal habits; solid columns (SC), aggregate of solid columns (ASC) and a general habit mix (GHM), for wavelengths from 0.2 to 100 µm, for effective diameters from 20 to 120 µm.

REFERENCES

Baum, B.A., P. Yang, A.J. Heymsfield, A. Bansemer, B.H. Cole, A. Merrelli, C. Schmitt and C. Wang, Ice cloud single-scattering property models with the full phase matrix at wavelengths from 0.2 to 100 µm. doi:10.1016/j.jqsrt.2014.02.029, 2014.

Canas, A.A., Murray J.E., Harries J.E., The Tropospheric Airborne Fourier Transform Spectrometer, SPIE, 3220, pp91-102,1997.

Marenco, F., Capabilities and operation of the FAAM EZlidar. Met Office OBR Tech. Note. NO. 79, 2010.

O'Shea, S.J., and 12 co-authors. Airborne observations of the microphysical structure of two contrasting cirrus clouds. J. Geophys. Res. Atmos., 121, 13510-13536, doi:10.1002/2016/D025278, 2016.

Poulsen, C. A., Siddans, R., Thomas, G. E., Sayer, A. M., Grainger, R. G., Campmany, E., Dean, S. M., Arnold, C., and Watts, P. D.: Cloud retrievals from satellite data using optimal estimation: evaluation and application to ATSR, Atmos. Meas. Tech., 5, 1889-1910, https://doi.org/10.5194/amt-5-1889-2012, 2012.

Vaisala, Advanced AVAPS System for Airborne Weather Research, 1999.

Wilson, S.H.S, Atkinson, N.C and Smith, J.A., The Development of an Airborne Infrared Interferometer for Meteorological Sounding Studies. J. Atmos. Oceanic Tech., 16, 1912-1927, 1999.

This work is funded by the European Space Agency, under reference 4000124917/18/NL/IA.

PRELIMINARY RESULTS FOR CASE STUDIES 1 & 3: Simulated TAFTS and ARIES brightness temperature spectra

CASE 1 (τ_{355nm}≈0.58, z_{cloud}=6.2-8.9 km)

Initial attempts to match the ARIES spectra yielded simulations that were around 5K too warm across the 750 to 1250 cm^{-1} atmospheric window. Increasing the optical depth by 50% yielded agreement to within the uncertainties of the ARIES spectra (see figure 7), and for the ASC habit with an effective radius of 25 µm.

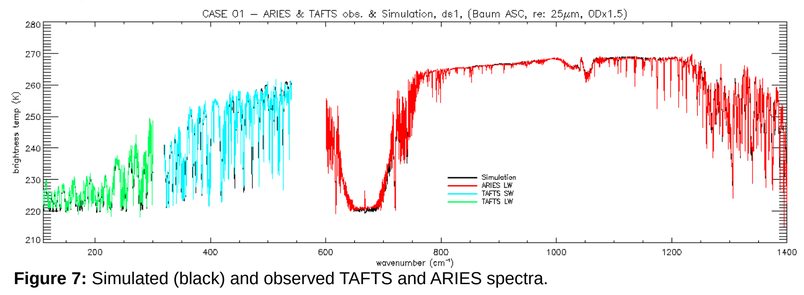

Figure 7: Simulated (black) and observed TAFTS and ARIES spectra.

Simulations were performed for a range of crystal habits and particle sizes which demonstrate those spectral regions in the FIR that may provide unique information on crystal habit and size when compared to the mid-IR alone (figure 8).

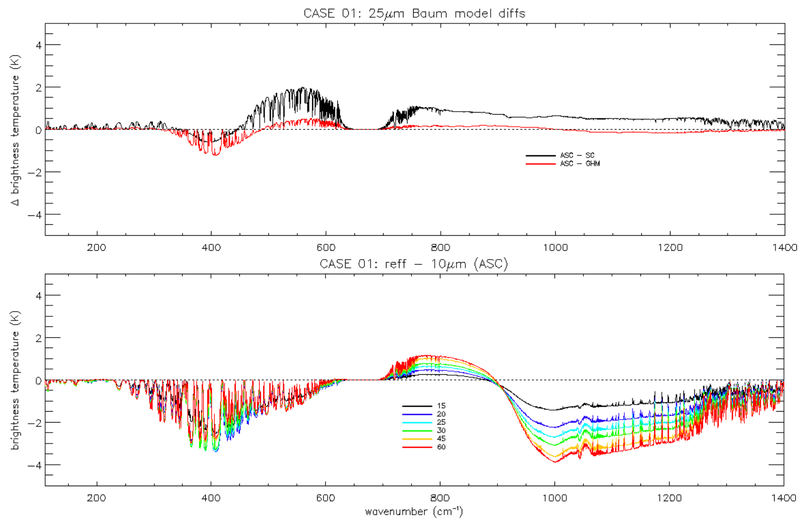

Figure 8: Top: Spectral differences due to variation in crystal habits compared to ASC. Bottom: Sensitivity to particle mean effective radius for sizes 15 to 60 µm compared to 10 µm for ASC.

CASE 3 (τ_{355nm}≈0.80, z_{cloud}=6.0-8.9 km)

Simulations were again focussed on providing the closest match to the ARIES spectra. For this case, increasing the optical depth by 20% (within lidar extinction profile uncertainties) yielded agreement to within the uncertainties of the ARIES spectra (see figure 9) which are of the order of 1K. Significant differences are seen between the simulation and the observed TAFTS spectra in spectral regions that may be particularly sensitive to crystal habit compared to the mid-IR (see figure 10).

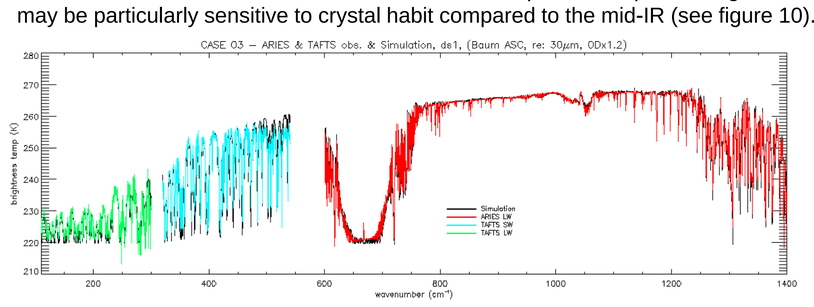

Figure 9: Simulated (black) and observed TAFTS and ARIES spectra.

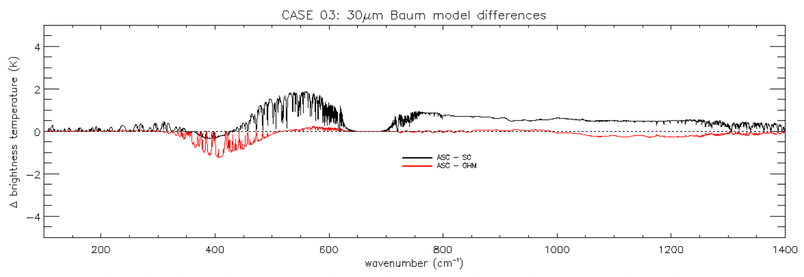

Figure 10: Top: Spectral differences due to variation in crystal habits compared to ASC.

Note: These preliminary simulations have been performed at a relatively low spectral resolution (0.5 cm^{-1}) – hence differences between simulations and observations are not shown. However, these simulations are being repeated at high spectral resolution, and it is evident even from these coarse resolution simulations that there are significant differences between the simulated and observed spectra in the FIR for well matched cases in the mid-IR.

Inverse modelling approach using ORAC

Oxford-RAL Retrieval of Aerosol and Cloud (ORAC), Poulsen 2012, is a state-of-the-art optimal estimation based retrieval model and forms part of the Community Cloud Code for Climate (CC4CL). It is routinely used to retrieve cloud properties from a number of satellite instruments using mid-IR and visible bands and is part of ESA's Climate Change Initiative on clouds. ORAC will be developed to perform retrievals of cirrus optical thickness, effective radius and cloud height using specific additional narrow band FIR channel data provided by TAFTS observations, along with mid-IR channels extracted from ARIES spectra. An example of ORAC's current capability, using MODIS collection 061 data from an overpass at 10:40 UTC on the 13th March 2015, is shown in figure 11. The cloud optical thickness ($\tau_{0.55}$≈ 1), cloud top height (z_{top}≈7km) and cloud effective radius (r_{eff}≈30µm) show promising agreement with the observations and the forward modelling approach.

Figure 11: Top: (i) left: MODIS false colour image, (ii) right: retrieved cloud optical thickness (0.55µm). Bottom: (i) left: cloud top height, (ii) cloud effective radius .